Soft Comput (2017) 21:7083–7098
DOI 10.1007/s00500-016-2251-6

METHODOLOGIES AND APPLICATION

Optimization of friction stir welding process parameters using soft computing techniques

Nizar Faisal Alkayem[1] · **Biswajit Parida**[1] · **Sukhomay Pal**[1]

Published online: 5 July 2016

Abstract In welding processes, desired weld quality is highly dependent on the selection of optimal process conditions. In this work, the influence of input parameters of friction stir welding process is studied using Taguchi method and full factorial design of experiment. The experimental data set is used to develop multilayer feed-forward artificial neural network (ANN) models using back-propagation training algorithm. These models are used to predict weld qualities as a function of eight process parameters. The weld qualities of the welded joint, such as ultimate tensile strength, yield stress, percentage elongation, bending angle and hardness, are considered. In order to offline optimize these quality characteristics, four evolutionary algorithms, namely binary-coded genetic algorithm, real-coded genetic algorithm, differential evolution and particle swarm optimization, are coupled with the developed ANN models. The optimized quality characteristics obtained from these proposed techniques are compared and verified with experimental results.

Keywords Friction stir welding · Artificial neural network · Genetic algorithms · Particle swarm optimization · Differential evolution

Communicated by V. Loia.

✉ Sukhomay Pal
spal@iitg.ernet.in

[1] Department of Mechanical Engineering, IIT Guwahati, Guwahati 781039, India

1 Introduction

Friction stir welding (FSW) is a solid-state joining process which was introduced in 1991 by Thomas et al. (1991). It is usually used for welding soft metals like aluminum, copper. The advantage of FSW process is that the welding is performed below the melting temperature, which does not lead to crack formation, solute redistribution and porosity, right after joining (Neto and Neto 2013; Mishra and Mahoney 2007). The FSW process uses a cylindrical tool with a profiled pin at the end. The tool is rotated and moved with a constant speed along the joint line. This movement causes plastic deformation and material mixing of the workpiece along the weld line which may lead to excellent welded joint (Neto and Neto 2013). The weld quality is usually evaluated by many characteristics like tensile strength, yield stress, elongation, hardness. These quality characteristics are controlled by a number of process parameters like plunging depth, tool rotation speed, tool geometry, shoulder diameter, pin diameter, tool pin length, dwell time. To obtain high weld quality, it is important to select optimal process parameter setting. This selection is not easy, because the number of parameters involved is large and the relationships between them and the output parameters are nonlinear and complex. Hard computing techniques require precise analytical model and lot of computation time. This makes it difficult to implement, especially when it is coupled with optimization techniques. Therefore, it is more preferable to implement soft computing techniques for the optimization of FSW process.

Recent studies attempted to model FSW process using artificial neural networks (ANNs). Boldsaikhan et al. (2011) studied wormhole defect in FSW process. They used back-propagation algorithm to train ANN model for classification of the feedback forces frequency patterns as indicators for wormhole defect. Lakshminarayanan and Balasubramanian

(2009) focused on estimation of ultimate tensile strength in FSW of Al alloy. They found that ANN modeling was more accurate compared to response surface methodology. Buffa et al. (2012) combined ANN model with a finite element model (FEM) for FSW of Ti–6Al–4V alloy. The model could predict the microhardness as well as the microstructure of the welded joints. Okuyucu et al. (2007) used ANN model to predict the mechanical properties of FSWed joints by considering only two input parameters (welding speed and tool rotation speed). Fratini et al. (2009) developed ANN model coupled with FEM model for estimation of average grain size of FSWed joints. Ghetiyaa and Patel (2014) developed ANN model for the prediction of tensile strength of Al alloy in FSW process. From the literature, it is found that researchers have successfully used ANN models to correlate the input and output relationship in FSW process.

Evolutionary algorithms simulate Darwin's principle of evolution to construct powerful search and optimization algorithms. Genetic algorithms (GAs) have been used as an optimization tool in various problem domains (Deb 2001). Kennedy and Eberhart (1995) proposed an optimization algorithm to simulate the behavior of flocks with particle swarm optimization (PSO). Storn and Price (1997) proposed differential evolution (DE) algorithm which is a fast and efficient population-based optimization algorithm.

Few attempts were made to apply evolutionary algorithms for optimization of the FSW process. Shojaeefard et al. (2013) utilized back-propagation training algorithm to develop ANN model for FSW process and multi-objective particle swarm optimization to optimize the mechanical properties. For the optimization problem, they considered only two inputs, namely rotational speed and welding speed, and two weld qualities, namely tensile strength and hardness of the welded joint. Tutum and Hattel (2010) were concerned about multi-objective optimization of residual stresses and production efficiency in FSW process. They developed thermomechanical model and applied NSGA-II for optimization. Shojaeefard et al. (2014) developed ANN model for FSW of AA5083 Al alloy by using back-propagation training algorithm. They used NSGA-II for optimization of two input parameters with three outputs. From the literature, it can be seen that number of inputs and outputs parameters considered for optimization of FSW process are less. But for effective application of FSW, it is important to consider all significant input and output parameters in the optimization process to ensure best weld quality.

In this work back-propagation training algorithm is utilized to develop ANN models to correlate the input–output parameters of FSW process. Four optimization techniques, namely binary-coded GA, real-coded GA, DE and PSO, are applied on the ANN models to obtain the optimum input parameters' settings offline. The results obtained from those algorithms are compared to determine the best optimization algorithm. Two cases are considered; the first one is maximization of mechanical properties of the welded joint, and the other is the optimization of desired weld quality parameters. Experiments are conducted to confirm the predicted results.

2 Experimental details

2.1 Experimental approach and results

In this work commercially available 6-mm-thick aluminum plates are used for experimentation purpose. The plates are cut and machined to rectangular pieces of 200 × 100 mm for joining purpose. But joints are prepared by FSW process. The chemical composition and mechanical properties of the plates are given in Table 1. The selection of appropriate tool material for carrying out FSW is an important issue. The FSW tool should withstand the vertical pressure and torque applied to it and should not wear out easily. Stainless steel (SS-310) is used as tool material because of its excellent properties at high temperature. A vertical milling machine is used to carry out the welding process with the specifications of spindle speed: 12 steps (50–1500 rpm), table feed: 8 steps (22–555 mm/min), main motor power: 5.5 kW, table motor power: 0.75 kW.

Initially, a list of all possible process parameters is prepared. Depending on the machine flexibility and setup limitations, the number is narrowed down to eight. The parameters considered in the present work are plunge depth (PD), tool rotational speed (RPM), welding speed (WS), tool geometry (TG), shoulder diameter (SD), pin diameter (PnD), tool pin length (TPL) and dwell time (DT). Four different tool geometries are used: straight cylindrical (SC), tapered cylindrical (TC), square (SQ) and threaded (THRD).

Table 1 Chemical composition and mechanical properties of the base material

Chemical composition (wt%)	Cu	Si	Fe	Al
	0.05	0.2	0.1	Balance
Mechanical properties	Ultimate tensile strength (MPa)	Yield strength (MPa)	% Elongation	
	153.05	84.93	33.04	

For the present investigation 59 experiments have been conducted, as shown in "Appendix, Table 11." Out of these 59 experiments the first 32 experiments are based on Taguchi's L_{32} orthogonal array (OA) design of experiment. In L_{32} OA design, plunge depth is varied in two levels and other seven parameters are varied in four levels. Initial trial runs show that the working range of PD is less due to which it has been varied in two levels. The next 27 experimental data sets are based on full factorial experimental design in which three process parameters (TG, RPM and PnD) are varied in three levels.

The plates to be joined are clamped in such a way that the plate movement is completely restricted under vertical as well as translational forces exerted by the tool. The tool rotation speed and traverse speed of the bed are set before each run of welding. Forty-one numbers of tools having different shapes and dimensions are fabricated in house to conduct the experiments. The welded plates are cut as per the diagram shown in Fig. 1a. Then the tensile specimens are prepared as per the American Society for Testing of Materials (ASTM E8) guidelines. The tensile, bending and hardness specimens are shown in Fig. 1b–d, respectively. Tensile tests are carried out in a digitally controlled closed loop servo hydraulic dynamic testing machine (Make: INSTRON, Model: 8801). The measured weld quality values of each welding condition corresponding to the parameter settings mentioned in Table 11 are given in "Appendix, Table 12." Two types of bend tests are carried out, namely root and face bend test to achieve accurate bending angle. Hardness values are measured at three different layers across the material thickness direction at 1, 2.5 and 4 mm distance from the top surface of the weld, respectively. Total 15 points are considered for nugget zone hardness, and their average value is considered for analysis. The various weld quality characteristics considered for optimization are ultimate tensile strength (UTS in MPa), yield strength (YS in MPa), ductility (% Elng.), bending angle (BA in degree) and nugget zone hardness (HRD in HV).

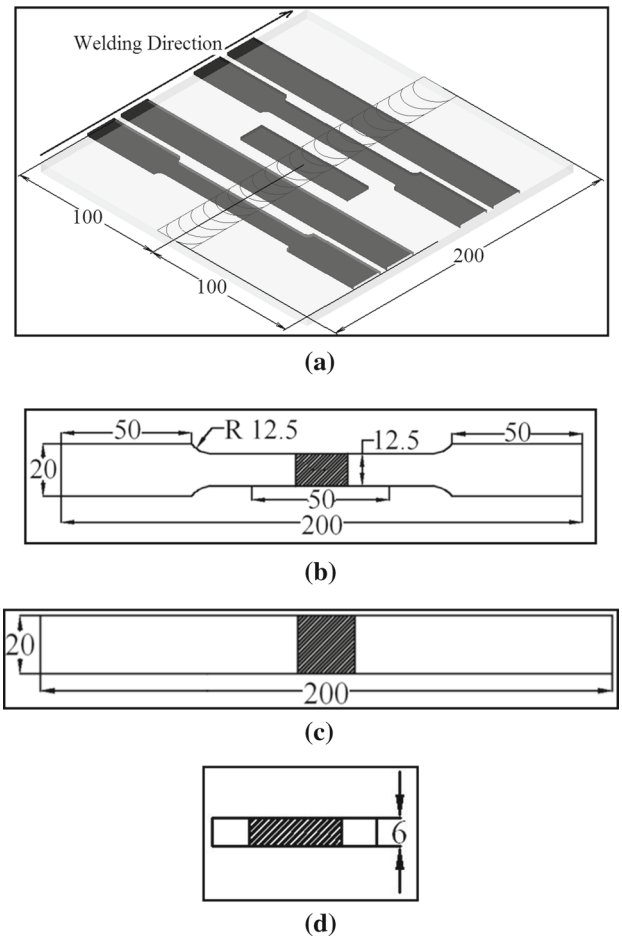

Fig. 1 Schematic diagrams of **a** position of extraction of tensile, bending and hardness specimens, **b** tensile, **c** bending, **d** microhardness specimen dimensions (all the above-mentioned dimensions are in mm)

2.2 Contribution of process parameters on the weld qualities

Analysis of variance (ANOVA) is applied to identify the effects of individual input parameter on the weld qualities. The contribution of each process parameter on the different weld quality parameters is calculated and is shown in Table 2. From the ANOVA results (Table 2), it is found that measured weld qualities are mostly influenced by RPM, TG and PnD. The most contributing parameter is RPM for UTS having the contribution of 29.67 %. This is because RPM is responsible of overall material mixing in both the surface level and along the thickness direction of the workpiece. The next most influencing parameters are TG and PnD having 21.85 and 21.07 % contributions, respectively. These two parameters are responsible for the material mixing along the thickness of the workpiece. Similarly for YS the contribution of the above three parameters are 26.34, 19.26 and 16.63 %, respectively.

Table 2 Percentage contribution of each input parameter on the different weld qualities

	Percentage contribution (%)				
	UTS	YS	% Elong.	BA	HRD
Input parameters					
PD	0.09	0.09	0.28	4.53	6.13
RPM	29.67	26.34	16.33	15.89	6.82
WS	1.29	3.28	2.23	5.04	9.88
TG	21.85	19.26	20.89	12.18	23.58
SD	1.75	6.34	3.56	11.04	4.78
PnD	21.07	16.63	38.65	28.63	3.64
TPL	2.40	5.10	2.88	2.86	11.09
DT	6.15	7.88	1.20	1.26	10.08

For bending test, all the good joints are bent up to 140° without any visible defect (or crack formation). The PnD is found to be the most important factor for bending angle as well as % elongation having contribution of 28.63 and 38.65 %, respectively. RPM and TG are found to be the next influencing factors. It is also found that RPM, TG and PnD parameters have the most significant effect on the considered weld qualities, whereas other considered parameters do not have significant effect on the weld qualities.

3 Modeling of weld quality characteristics using ANN

ANN approach of modeling can be performed using experimental data without making any simplifying assumptions. A detailed description of the operating principles of ANN can be referred to the relevant technical book (Haykin 2003). A schematic representation of a fully connected multilayer neural network (MLNN) architecture is shown in Fig. 2. The network consists of three layers, namely input layer containing different input neurons/parameters, hidden layer containing hidden neurons and output layer containing output neuron(s)/parameter(s). The information is received by the input layer from an external source, which is then multiplied by the interconnection weights between it and the adjacent hidden layer. The products are summed up and then modified by an activation function. In this case log-sigmoid function is chosen as the activation function for both the layers. These modified values become the outputs from the hidden layer and input signals for the next layer and finally reach to the output layer. Then, the procedure is terminated at the external receptor node(s).

In the present work, a C code for a multi-neurons, single hidden layer ANN model is developed for mapping the FSW process parameters to the weld quality parameters. The developed model is trained in a supervised manner using batch mode of training with error back-propagation algorithm. The model is trained on randomly selected data set of 40 input–output data pairs. Initial weight values are chosen randomly between ±0.9, and the bias value at the input layer is taken as zero and those for hidden and output layers as one. All the input and output variables are normalized between 0.1 and 0.9. The training objective is the mean square error (MSE) minimization by updating the network parameters through the gradient descent method.

$$\mathrm{MSE}(n) = \frac{1}{2PN_O} \sum_{p=1}^{P} \sum_{k=1}^{N_O} \left(O_{Ok}^{p}(n) - T_k^p\right)^2 \tag{1}$$

where MSE(n) is the MSE at the nth iteration, P is the total number of training patterns, N_O is the number of neurons in the output layer, $O_{Ok}^{p}(n)$ is the output of the kth output neuron for the pth pattern at the nth iteration and T_k^p is the desired kth output for the pth pattern. The performance of neural network depends on number of hidden neurons (NHN), learning rate (η) and momentum coefficient (α). Therefore, several combinations should be tried out to choose an optimal combination. To develop optimal ANN models for UTS, YS, % Elong., BA and HRD, the NHN, η and α values are varied within a range of 5–30 and 0.05–0.95, respectively. This process is carried

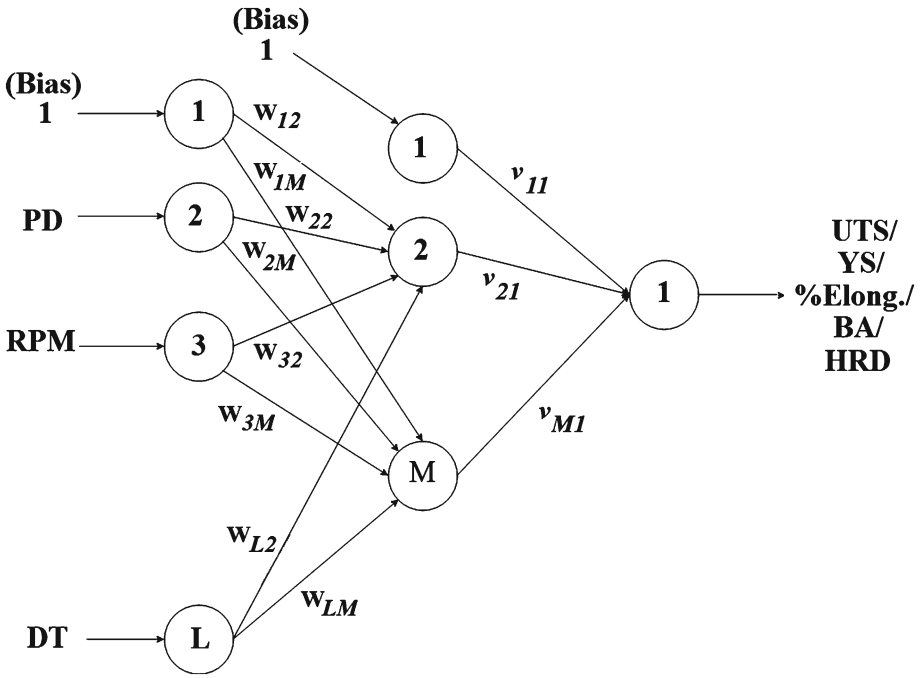

Fig. 2 Architecture of multilayer neural network (L and M are number of input and hidden neurons, respectively)

Table 3 Actual values, ANN predicted values and corresponding percentage errors for the testing cases

	UTS			YS			% Elng.			BA			HRD		
	Actl.	Predicted	% Error	Actl.	Predicted	% Error	Actl.	Predicted	% Error	Actl.	Predicted	% Error	Actl.	Predicted	% Error
1	133.9	132.11	−1.326	86.82	82.24	−5.273	15.18	14.02	−7.618	140	143.14	2.244	49.93	56.37	12.904
2	124.3	124.89	0.493	70.59	71.67	1.523	12.71	14.60	14.863	140	134.08	−4.225	54.57	54.66	0.158
3	129.6	127.22	−1.852	78.97	84.41	6.892	13.96	13.73	−1.671	140	140.37	0.267	53.27	55.72	4.608
4	133.1	133.57	0.388	85.24	97.49	14.366	15.4	14.95	−2.924	140	148.90	6.358	50.93	54.67	7.352
5	127.5	123.38	−3.216	75.07	69.66	−7.201	14.01	15.37	9.710	140	141.28	0.916	57.31	52.70	−8.053
6	132.0	135.10	2.315	83.37	91.22	9.420	15.58	15.32	−1.658	140	143.17	2.266	50.32	56.38	12.040
7	118.5	116.70	−1.521	66.57	71.42	7.287	12.05	11.86	−1.542	140	118.59	−15.295	56.37	56.22	−0.261
8	131.6	126.98	−3.510	84.17	76.59	−9.009	14.34	14.50	1.106	140	145.00	3.571	57.93	54.35	−6.184
9	125.8	128.29	1.996	74.71	81.39	8.935	13.88	15.07	8.584	140	139.03	−0.690	58.4	53.30	−8.738
10	128.5	131.33	2.184	78.8	85.96	9.087	14.46	13.24	−8.446	140	140.25	0.176	55.38	58.66	5.924
11	127.7	121.25	−5.027	75.73	69.73	−7.918	10.26	12.60	22.851	140	123.66	−11.674	56.11	57.06	1.686
12	133.6	134.54	0.702	85.65	93.36	9.001	15.2	15.94	4.864	140	147.50	5.356	57.47	58.88	2.459
13	139.7	138.01	−1.231	89.25	104.46	17.044	16.15	17.00	5.289	140	151.23	8.023	58.1	58.43	0.569
14	131.3	132.07	0.575	84.1	89.20	6.061	15.06	15.71	4.344	140	143.67	2.625	56.09	59.05	5.274
15	135.9	138.09	1.606	90.74	98.84	8.932	15.86	16.06	1.267	140	144.42	3.157	57.61	60.39	4.824
16	136.2	139.93	2.724	87.13	99.46	14.156	16.15	15.63	−3.217	140	141.64	1.168	53.56	56.36	5.223
17	132.2	129.85	−1.789	87.59	85.77	−2.082	14.62	13.89	−4.982	140	141.59	1.134	57.64	57.57	−0.121
18	135.1	133.95	−0.853	89.25	91.29	2.281	15.5	13.25	−14.501	140	136.37	−2.594	59.17	59.89	1.218
19	130.5	134.38	2.950	93.41	95.57	2.310	15.24	12.30	−19.293	140	127.44	−8.972	54.07	61.80	14.289
Mean absolute percentage error			1.908			7.830			7.302			4.248			5.362

out separately for each output. After training the developed model, the remaining nineteen data sets are used to test the network performance. The ANN predicted values and percentage errors in prediction are shown in Table 3. From the predicted values, it is found that the average errors in prediction of joint properties are within 10 % deviation. So the developed model can be used effectively for prediction of weld quality in FSW process.

4 Optimization procedures

4.1 Genetic algorithms

GAs are search and optimization procedures that are motivated by the principles of natural evolution. In binary GA, the input parameters of the optimization problem are represented by binary strings (Deb 2001). In other words, initially a population of random strings of bits is created. To make sure that the population satisfies the problem bounds, Eq. (2) is applied

$$x_i = x_i^{\min} + \frac{x_i^{\max} - x_i^{\min}}{2^{l_i} - 1} \mathrm{DV}(s_i) \tag{2}$$

where l_i the string length is used to code the ith parameter and $\mathrm{DV}(s_i)$ is the decoded value of the string s_i. l_i can be obtained from the following relation with desired accuracy (ε):

$$l_i = \log_2 \left(\frac{x_i^{\max} - x_i^{\min} + 1}{\varepsilon} \right) \tag{3}$$

In order to decide the survival of each individual, the next necessary procedure is fitness evaluation, by means of the objective function and constraints. If there is absence of constraints, the fitness is made equal to the objective function value.

The objective function that is used in this work is created by using weighted sum method. The weighted sum method converts the set of objectives into one single objective by the multiplication of each objective with a specific weight which depends on the importance of the objective. The objective function considered in this work is defined as:

$$\begin{aligned} f_i = {} & 0.25\mathrm{UTS}_i + 0.25\mathrm{YS}_i \\ & + 0.2\mathrm{Elong}_i + 0.15\mathrm{BA}_i + 0.15\mathrm{HRD}_i \end{aligned} \tag{4}$$

where f_i is the objective function value or the fitness of the ith individual in the population; UTS_i, YS_i, Elong_i, BA_i and HRD_i are the ultimate tensile strength, yield stress, % elongation, bending angle and hardness values corresponding to the ith individual in the population. The flowchart of the neuro-GA model is shown in Fig. 3.

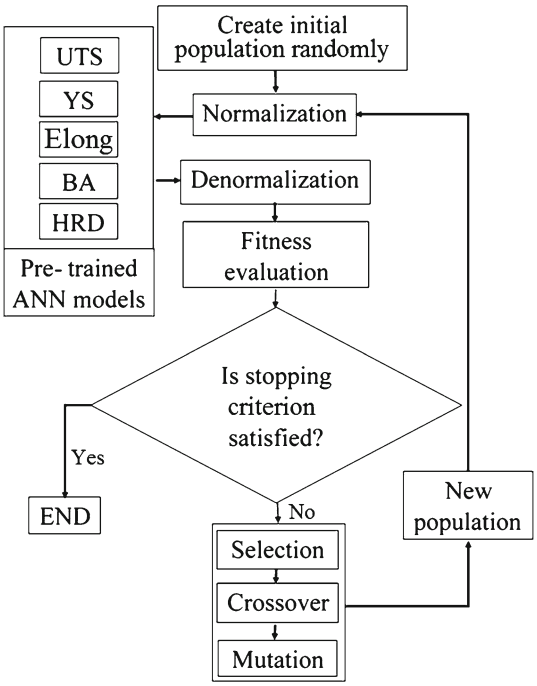

Fig. 3 Flowchart of neuro-GA

GAs are dependent on three main parameters; these are selection, crossover and mutation (Deb 2001). In this work tournament selection method is used with size of 5. After selection of good individuals, crossover and mutation operations are performed. Crossover gives the GA its exploration ability, whereas mutation gives exploitation ability. In this work uniform crossover and global mutation are applied.

In real-coded GA instead of binary strings, real values are used directly. Similar operators to that in binary-coded GA can be used. In this work tournament selection, simulated binary crossover (SBX) and random mutation are performed.

4.2 Differential evolution

DE is a very simple population-based optimization technique (Storn and Price 1997). The population is composed of a set of random vectors. The basic concept of DE relies on selecting two random vectors from the population and finding the difference between them. This difference is then multiplied with a certain weight and added to a third random vector. This operation is called mutation. For all the target vectors x_i, the mutant vector v_i is calculated by using Eq. (5)

$$v_i = x_{r_1} + F\left(x_{r_2} - x_{r_3}\right) \tag{5}$$

where x_{r_1}, x_{r_2} and x_{r_3} are randomly chosen vectors and F is a constant factor $\in [0, 2]$.

Another way to create the mutant vector is to replace x_{r_1} by x_{best} which is the best vector obtained so far during the

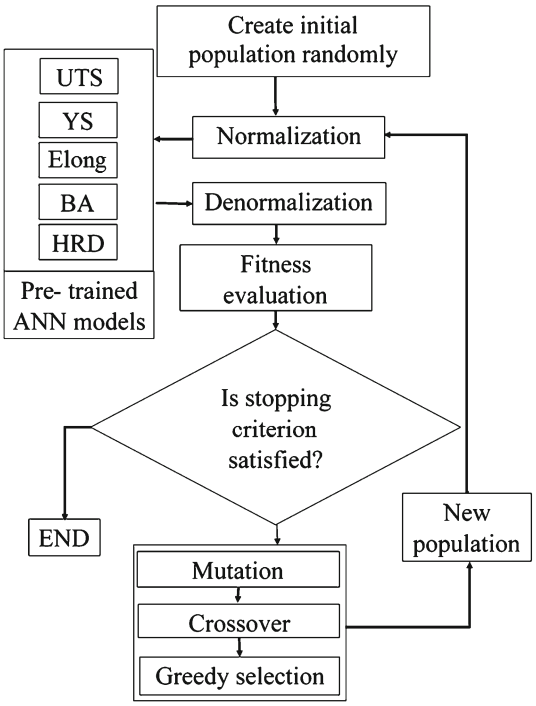

Fig. 4 Flowchart of neuro-differential evolution

evolution. And to increase diversity, two difference vectors are used in this work as it is shown in Eq. (6)

$$v_i = x_{\text{best}} + F\left(x_{r_1} - x_{r_2} + x_{r_3} - x_{r_4}\right) \tag{6}$$

where x_{r_1}, x_{r_2}, x_{r_3} and x_{r_4} are randomly chosen vectors.

To perform crossover, DE generates trial vectors ($u_{ij,G+1}$) and mixes them with the original target vectors. This process is shown in Eq. (7)

$$u_{ij,G+1} = \begin{cases} u_{ij,G+1} & \text{if } r \le pc \quad \text{or } j = \delta \\ x_{ij,G} & \text{if } r > pc \quad \text{or } j \ne \delta \end{cases} \tag{7}$$

where r is a random number $\in [01], \delta \in \{1, 2, \ldots, n\}$ randomly chosen index of any vector, G is the generation number, and pc is the crossover probability.

The last operator in DE is Greedy selection. If the trial vector $u_{i,G+1}$ results in better objective function value than the target vector $x_{i,G}$, then $x_{i,G+1}$ is set to $u_{i,G+1}$, otherwise, the old vector $x_{i,G}$ is retained. The flowchart of DE is shown in Fig. 4.

4.3 Particle swarm optimization

PSO is a population-based optimization algorithm. The population is constructed by random solutions named as particles. These particles move through the problem search space by utilizing some current optimal particles. In every iteration, each particle is updated by two other best particles, namely p-best which is the best performance of the corresponding

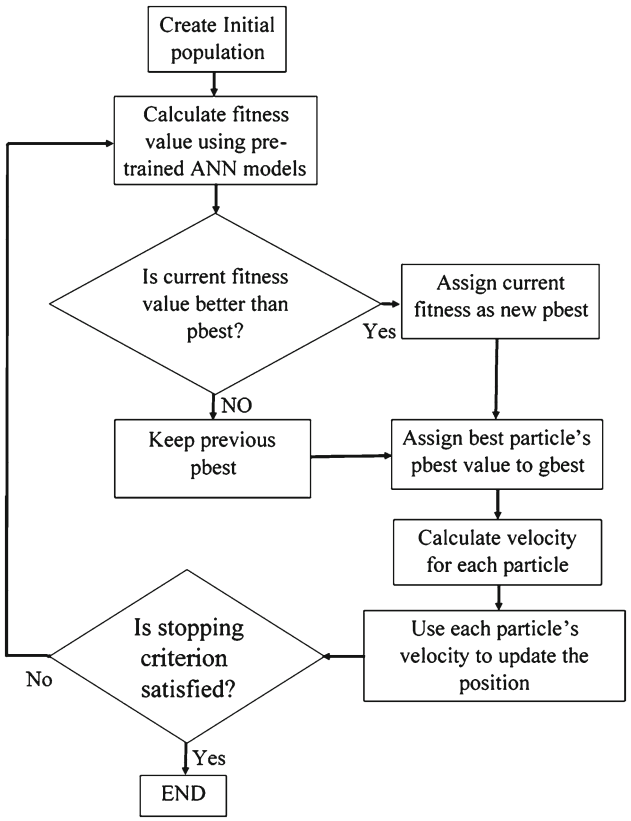

Fig. 5 Neuro-PSO flowchart

particle so far and the other is g-best which is the best value obtained from the whole population. After finding the two best values, the particle updates its velocity and positions until reaching the best solution. The position and velocity of particle are updated using following equations. The flowchart of PSO is shown in Fig. 5.

$$\text{par}_i^{(t+1)} = \text{par}_i^{(t)} + v_i^{(t+1)} \tag{8}$$

$$v_i^{(t+1)} = w_i v_i^{(t)} + c_1 r_1 (\text{pbest}^{(t)} - \text{par}_i^{(t)}) + c_2 r_2 (\text{gbest}^{(t)} - \text{par}_i^{(t)}) \tag{9}$$

where par_i^t is the ith particle at the tth iteration, $v_i^{(t)}$ is the velocity of the ith particle at the tth iteration, w_i is the inertia added to the ith particle, c_1 & c_2 are acceleration coefficients, and r_1 & r_2 are random numbers $\in$ [0 1].

5 Results and discussion

5.1 Determination of optimal input parameters for maximization of weld qualities

Initial population of solutions is created randomly and normalized between [0.1 0.9] and fed to the pretrained ANN models. The response characteristics are computed inside

Table 4 Bounds and number of bits used in binary-coded GA

Parameter	Lower bound	Upper bound	String length
Plunging depth (mm)	0.09	0.15	11
Tool rotation speed (rpm)	600	1500	5
Welding speed (mm/s)	63	200	18
Tool geometry	1	4	2
Shoulder diameter (mm)	20	35	14
Pin diameter (mm)	5	8	12
Tool pin length (mm)	5.2	5.8	11
Dwell time (s)	10	25	14

Table 5 Parameters of binary-coded GA computations

Operator	
Population size	50–500 in steps of 50
Selection process	Tournament selection
Crossover	Uniform crossover with probability between 0.1 and 0.95 in a step of 0.1
Mutation	Global mutation with probability between 0 and 0.95 in a step of 0.05

the ANN models, denormalized and fed to the four evolutionary algorithms mentioned in Sect. 4. The objective of these optimization algorithms is to find out the optimal input parameter settings for higher weld quality characteristics and to compare the performance of each of them.

In binary GA, 2 bits are chosen to represent four tool geometries (SC, TC, SQ and THRD) and 5-bit string for the tool rotation speed. The number of bits in each string of the input parameters with accuracy $\varepsilon = 0.001$ and the bounds of the input parameters are shown in Table 4. The parameters of binary-coded GA computations are shown in Table 5.

In GA, the performance of the algorithm is influenced by the population size, crossover and mutation probability. A large population size allows better exploration of the search space and reduces the chances of sticking in local optima. Large crossover and small mutation rates are better to maintain good convergence of the algorithm. The variations of the maximum objective function values with population size, crossover and mutation rates are shown in Fig. 6a–c. From the figures it is obvious that population size more than 200, crossover rate above 0.5 and mutation rate between 0.1 and 0.25 have the best objective function values. The convergence of the objective function value to the optimal solution with 200 population size, 0.9 crossover rate and 0.2 mutation rate is shown in Fig. 6d.

Similar analysis is done in the case of real-coded GA. The parameters of real-coded GA computations are shown in Table 6. The variations of the maximum objective function values with population sizes, crossover rates and mutation probabilities are shown in Fig. 7a–c. It can be seen that population size with 300 individuals and more, crossover rates higher than 0.8 and mutation rates between 0.15 and 0.3 are giving the best objective function values. The convergence of the objective function value to the optimal solution with 400 population size, 0.95 crossover rate and 0.2 mutation rate is shown in Fig. 7d.

In PSO, the performance of the algorithm is influenced by the population size, inertia component w and acceleration coefficients $c1$ and $c2$. A population size with more than 150 particles, inertia component less than 1.5, acceleration coefficient $c1$ more than 1 and $c2$ between 0.5 and 3.5 are found to give the best objective function values as it is shown in Fig. 8a–c. By running the algorithm with w equals to 0.9, 2 for $c1$ and $c2$, 150 population size and 200 iterations, the convergence of the objective function value to the optimal solution is shown in Fig. 8e.

In order to check the performance of DE algorithm, population size, F factor and crossover rate are varied. Form Fig. 9a–c, it can be seen that population size more than 150, F between 0.5 and 1.7, crossover rate more than 0.5 give the best objective function values. The convergence of DE algorithm with crossover rate of 0.5, F factor of 1.5 and population size of 150 is shown in Fig. 9d.

The comparative results of all the techniques used in this study are shown in Table 7. From the tabulated result it is found that real-coded GA, PSO and DE algorithms give better weld characteristics than binary-coded GA. Moreover, PSO gives the near optimal solution with a relatively low population size and iteration number. Approximately same optimum parameter settings are obtained from real-coded GA, DE and PSO. It is clear from Table 7 that low values of PD, WS, PnD and DT with large values of rotation speed, SD, TPL and THRD tool give the best weld quality. The reason can be explained by the excellent material mixing along the surface and thickness level of the weld joint and also the suitable heat characteristics which may produce high-quality joints after cooling. One confirmation experiment is conducted to con-

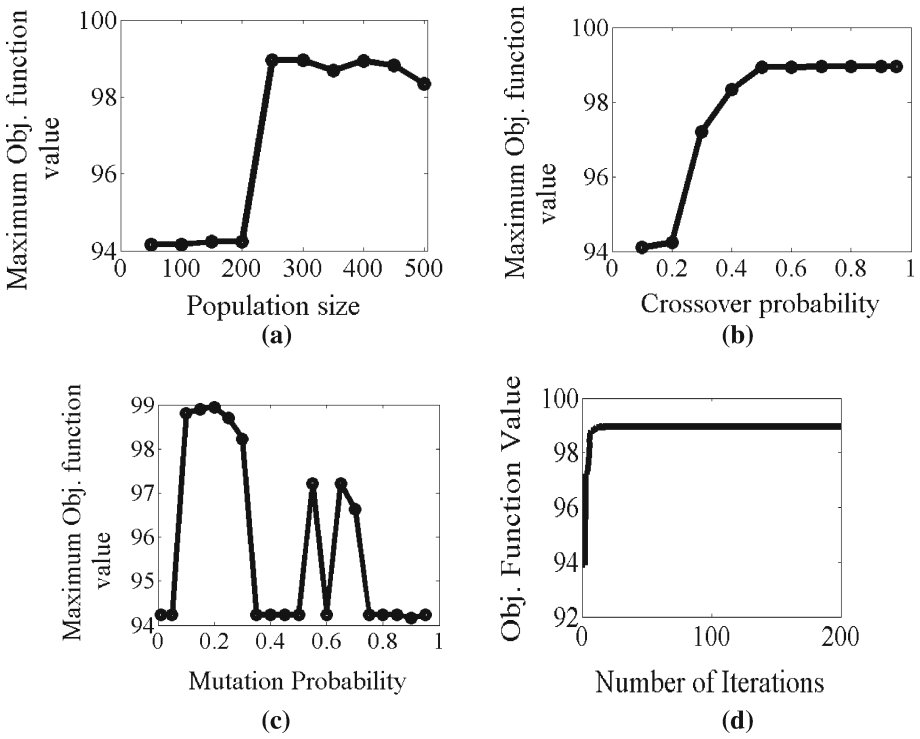

Fig. 6 Variation of maximum objective function value with: **a** population size, **b** crossover rate, **c** mutation rate in binary-coded GA, **d** the convergence of binary-coded GA algorithm

Table 6 Parameters of real-coded GA computations

Operator	
Population size	50–1000 in steps of 50
Selection process	Tournament selection
Crossover	SBX crossover with probability between 0.1 and 0.95 in a step of 0.1
Mutation	Random mutation with probability between 0 and 0.95 in a step of 0.05

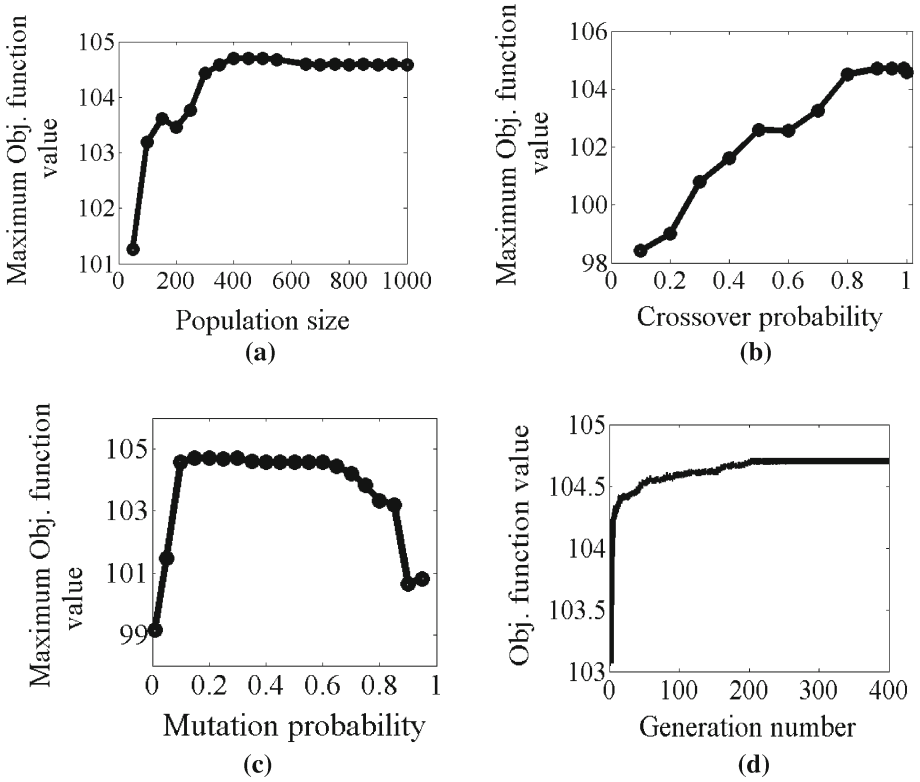

Fig. 7 Variation of maximum objective function value with: **a** population size, **b** crossover rate, **c** mutation rate in real-coded GA, **d** the convergence of real-coded GA algorithm

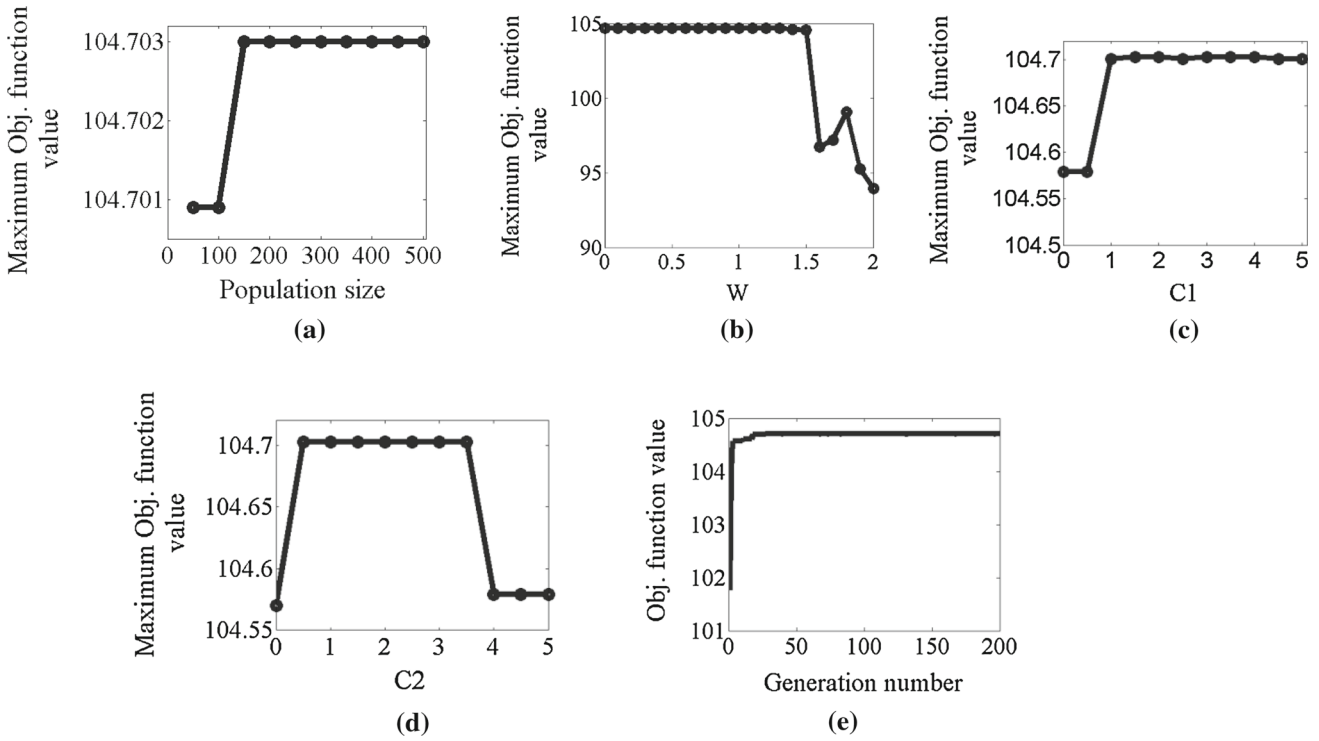

Fig. 8 Variation of maximum objective function value with: **a** population size, **b** inertia component, **c** coefficient $c1$ and **d** coefficient $c2$ using PSO, **e** the convergence PSO algorithm

Fig. 9 Variation of maximum objective function value with: **a** population size, **b** factor F and **c** crossover rate in DE, **d** the convergence of DE algorithm

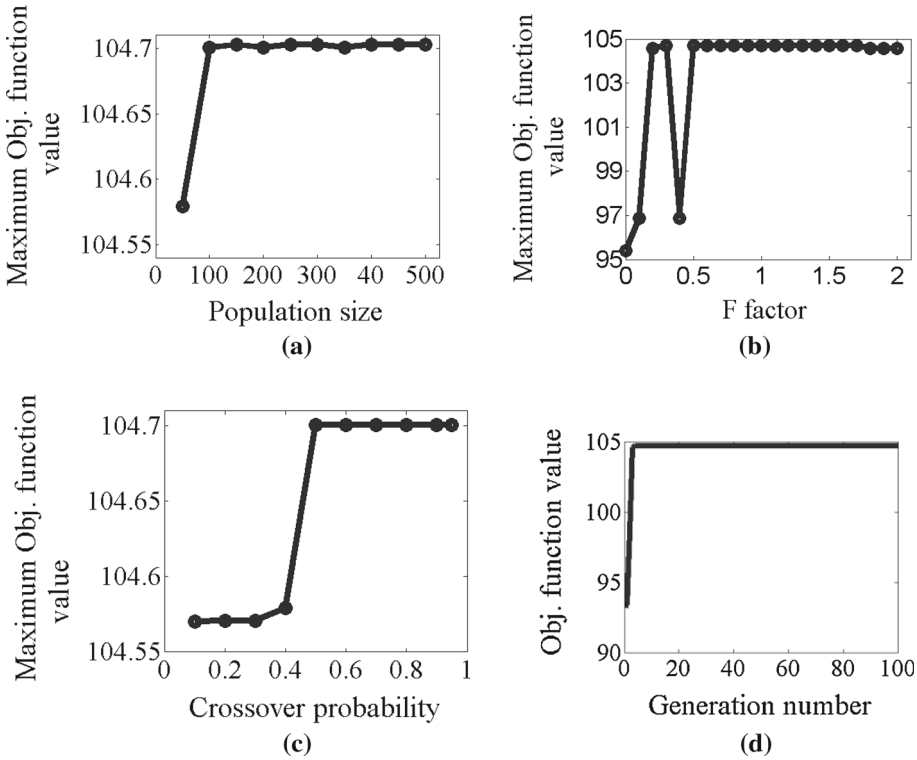

firm the best model predicted outputs. The optimum process parameters settings are rounded to near possible parameters in the FSW machine. The measured weld quality values are 145.38 MPa, 99.25 MPa, 19.98, 140° and 64.1 HV for UTS, YS, % Elong., BA and HRD, respectively. Mean absolute percentage error is 9.85 %. Even though the error is relatively high, the experiment has given good confirmation of the model predicted values.

Table 7 Results obtained from maximization of weld quality parameters

Parameter	Binary-coded GA	Real-coded GA	DE	PSO
Optimum input parameters				
Plunging depth	0.09	0.09	0.09	0.09
RPM	1035	1500	1500	1500
Welding speed	89.20	65.91	65.97	65.91
Toll geometry	SQR	THRD	THRD	THRD
Shoulder diameter	20.36	35	35	35
Pin diameter	7.53	5	5	5
Toll pin length	5.78	5.8	5.8	5.8
Dwell time	17	12	12	12
Model predicted outputs				
UTS	151.31	158.84	158.84	158.85
Yield stress	105.10	110.37	110.37	110.35
Elongation	15.34	24.68	24.68	24.69
Bending angle	152.14	153.70	153.70	153.70
Hardness	59.70	62.75	62.75	62.74
Objective function value	98.9458	104.703	104.703	104.703

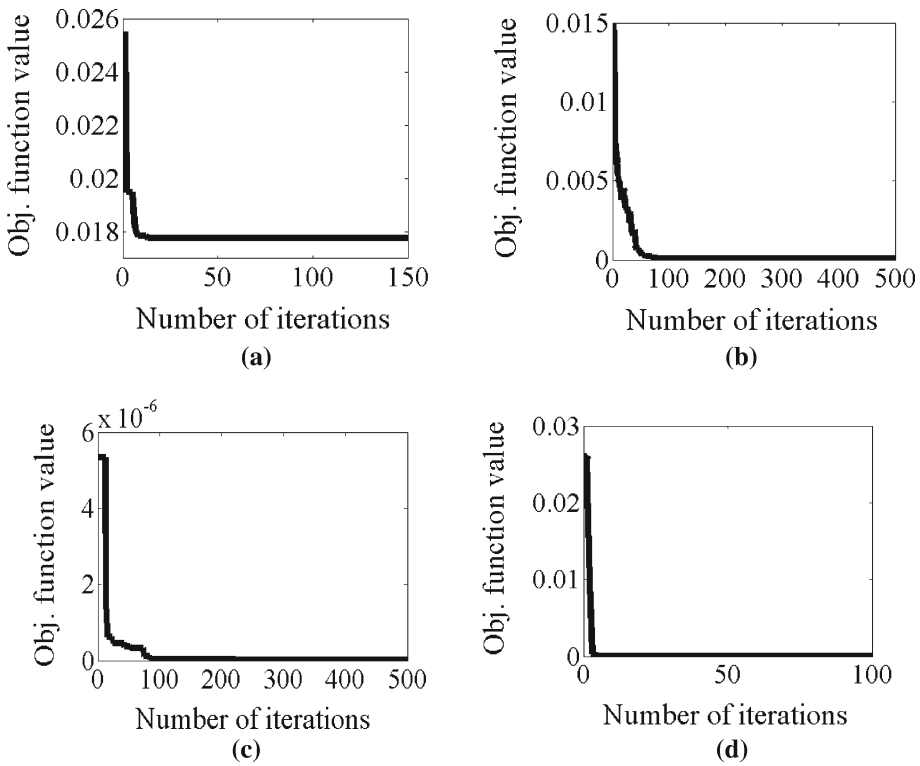

Fig. 10 Objective function value versus the iteration number for **a** binary-coded GA **b** real-coded GA, **c** DE and **d** PSO

Table 8 Desired weld quality parameters

	Desired quality parameters				
Parameter	UTS (MPa)	YS (MPa)	Elong. (%)	BA (°)	HRD
Target values	130	100	20	140	50

5.2 Determination of optimum input parameters setting for desired weld quality parameters

In the previous case (discussed in the Sect. 5.1) optimum process parameters settings have been determined for maximum weld quality characteristics. Other than maximization

Table 9 Optimized parameter settings with model predicted weld quality for the target value

Parameter	Binary-coded GA	Real-coded GA	DE	PSO
Optimum input parameters				
Plunging depth	0.10	0.10	0.10	0.10
RPM	832	601	600	600
Welding speed	82	63	63	63
Toll geometry	THRD	SQR	SQR	SQR
Shoulder diameter	25.9	20.4	20.1	20.0
Pin diameter	5.14	7.28	7.01	7.03
Toll pin length	5.51	5.80	5.80	5.80
Dwell time	14	23	23	23
Model predicted outputs				
UTS	132.82	133.95	129.90	130.46
Yield stress	94.67	98.41	100.58	100.55
Elongation	18.26	19.73	19.86	19.99
Bending angle	130	140	139	139
Hardness	57	51	51	51
Objective function value	0.006	2.76E−04	1.35E−04	1.22E−04

of weld quality parameters sometime desired weld quality values are also required. Therefore, for finding the optimum process parameters setting for desired (target) weld quality characteristics, following objective function is considered.

$$O_f(i) = w_1\left(\frac{\mathrm{UTS}_t - \mathrm{UTS}(i)}{\mathrm{UTS}_t}\right)^2 + w_2\left(\frac{\mathrm{YS}_t - \mathrm{YS}(i)}{\mathrm{YS}_t}\right)^2 + w_3\left(\frac{\%\,\mathrm{Elong}_t - \%\,\mathrm{Elong}(i)}{\%\,\mathrm{Elong}_t}\right)^2 + w_4\left(\frac{\mathrm{BA}_t - \mathrm{BA}(i)}{\mathrm{BA}_t}\right)^2 + w_5\left(\frac{\mathrm{HRD}_t - \mathrm{HRD}(i)}{\mathrm{HRD}_t}\right)^2 \quad 10 \tag{10}$$

where $O_f(i)$ is the value of the objective function of the ith individual in the population; UTS_t is the target (desired) value for the joint tensile strength; $\mathrm{UTS}(i)$ is the value of tensile strength of the ith individual; YS_t is the target value for the yield stress; $\mathrm{YS}(i)$ is the value of yield stress of the ith individual; $\%\,\mathrm{Elong}_t$ is the target value for elongation; $\%\,\mathrm{Elong}(i)$ is the % elongation value of the ith individual; BA_t is the target value for the bending angle; $\mathrm{BA}(i)$ is the bending angle value of the ith individual; HRD_t is the target value for the nugget zone hardness, $\mathrm{HRD}(i)$ is the experimental value for the nugget zone hardness of the ith individual in the population; w_1, w_2, w_3, w_4 and w_5 are weights that give different status or importance to each response. The responses evaluated in this work do not have equal importance. The most important response is the UTS, followed by the yield stress, elongation, bending angle and hardness. The weights are 0.25 for UTS and yield stress, 0.2 for elongation and 0.15 for bending angle and nugget zone hardness.

In this case, one arbitrary target value is considered. These desired weld quality parameters are shown in Table 8. Similar procedure to that performed for the first objective function (i.e., maximization of quality parameters) is performed to obtain best parameters for each proposed algorithm. The objective function (Eq. 10) value versus the iteration number for the four optimization techniques is shown in Fig. 10a–d. The optimum input parameter settings and model predicted outputs corresponding to the target value are shown in Table 9. It is clear that real GA, DE and PSO are able to find approximately the same near optimum weld characteristics which are better than binary GA. Nevertheless, PSO has the maximum convergence speed among the other algorithms which makes it the most preferable algorithm.

5.3 Confirmation results

To check the accuracy of the modeling and optimization procedure, two confirmation experiments are conducted. The input parameters are taken from Table 9 and rounded to the near possible parameters in the FSW machine. The first experiment is performed for checking the optimal solution of binary-coded GA for the target value. The second one is for checking the value obtained from real-coded GA, DE and PSO. Experimental weld characteristics with corresponding model predicted outputs and percentage errors are shown in Table 9. Experimental results for the target value in Table 10 show that the errors in both the experiments are less than 10 % which is acceptable. The model predicted weld quality parameters are also well close to the corresponding experimental results. Moreover, the second experiment gives better results (6.6 % error) which leads to the conclusion that results

Table 10 Comparison between experimental and model predicted weld characteristics

Cases	Optimization techniques		UTS	YS	% Elong.	BA (°)	HRD	Mean absolute errors (%)
Target value	Binary GA	Desirable values	130	100	20	140	50	8.5
		Experimental values	130.38	93.02	17.16	140	60.5	
		Percentage error (%)	+0.29	−6.98	−14.2	0	+21	
	RGA, DE and PSO	Desirable values	130	100	20	140	50	6.6
		Experimental values	121.71	92.38	16.5	140	50.7	
		Percentage error (%)	−6.38	−7.62	−17.5	0	+1.4	

obtained from real-coded GA, PSO and DE are more accurate.

From the aforementioned case studies, it can be recommended that PSO is more suitable for optimization of FSW process. This is mainly because it has showed the ability to find the optimal solutions for both the objective functions with less number of iterations (Figs. 9, 10) comparing to other three algorithms.

6 Conclusions

In the present work, the contribution of each FSW process parameter on weld qualities has been studied. ANOVA has showed that the most significant parameters on UTS, YS, ductility and BA are RPM, TG and PnD, whereas TG, TPL and DT are the most significant on HRD. Modeling and optimization of FSW process using ANN and four evolutionary algorithms have been also investigated. The search for the optimum is based on two cases. The first case is the maximization of an objective function, which takes into account the joint strength, yield stress, percentage elongation, bending angle and nugget zone hardness. The second case is the determination of optimum input parameter settings for desired weld quality values. For both the cases, it is found that the neuro-EA approach can be a powerful tool in welding process optimization with a relatively small experimental data set. PSO and DE are more suitable algorithms to apply because they are able to find the optimum values of the objective functions. Moreover, since PSO has given the optimum solution with less number of iterations, we can say that PSO is relatively the best optimization method for FSW process.

Acknowledgements The authors gratefully acknowledge the financial support provided by SERB (Science & Engineering Research Board), India (Grant No. SERB/F/2767/2012-13), to carry out this research work.

Compliance with ethical standards

Conflict of interest The authors declare that there is no conflict of interests regarding the publication of this paper.

Appendix

See Tables 11 and 12.

Table 11 Design matrix of experimental run

Exp. no.	PD	RPM	WS	TG	SD	PnD	TPL	DT
1	0.09	600	63	1	20	5	5.2	10
2	0.09	600	98	2	25	6	5.4	15
3	0.09	600	132	4	30	7	5.6	20
4	0.09	600	200	3	35	8	5.8	25
5	0.09	815	63	1	25	6	5.6	20
6	0.09	815	98	2	20	5	5.8	25
7	0.09	815	132	4	35	8	5.2	10
8	0.09	815	200	3	30	7	5.4	15
9	0.09	1100	63	2	30	8	5.2	15
10	0.09	1100	98	1	35	7	5.4	10
11	0.09	1100	132	3	20	6	5.6	25
12	0.09	1100	200	4	25	5	5.8	20
13	0.09	1500	63	2	35	7	5.6	25

Table 11 continued

Exp. no.	PD	RPM	WS	TG	SD	PnD	TPL	DT
14	0.09	1500	98	1	30	8	5.8	20
15	0.09	1500	132	3	25	5	5.2	15
16	0.09	1500	200	4	20	6	5.4	10
17	0.15	600	63	3	20	8	5.4	20
18	0.15	600	98	4	25	7	5.2	25
19	0.15	600	132	2	30	6	5.8	10
20	0.15	600	200	1	35	5	5.6	15
21	0.15	815	63	3	25	7	5.8	10
22	0.15	815	98	4	20	8	5.6	15
23	0.15	815	132	2	35	5	5.4	20
24	0.15	815	200	1	30	6	5.2	25
25	0.15	1100	63	4	30	5	5.4	25
26	0.15	1100	98	3	35	6	5.2	20
27	0.15	1100	132	1	20	7	5.8	15
28	0.15	1100	200	2	25	8	5.6	10
29	0.15	1500	63	4	35	6	5.8	15
30	0.15	1500	98	3	30	5	5.6	10
31	0.15	1500	132	1	25	8	5.4	25
32	0.15	1500	200	2	20	7	5.2	20
33	0.09	600	98	1	25	5	5.7	15
34	0.09	1100	98	1	25	5	5.7	15
35	0.09	1100	98	3	25	6	5.7	15
36	0.09	600	98	3	25	5	5.7	15
37	0.09	1100	98	1	25	6	5.7	15
38	0.09	1100	98	1	25	7	5.7	15
39	0.09	600	98	2	25	6	5.7	15
40	0.09	815	98	1	25	7	5.7	15
41	0.09	815	98	2	25	7	5.7	15
42	0.09	600	98	1	25	6	5.7	15
43	0.09	815	98	2	25	5	5.7	15
44	0.09	1100	98	2	25	5	5.7	15
45	0.09	600	98	1	25	7	5.7	15
46	0.09	815	98	2	25	6	5.7	15
47	0.09	815	98	1	25	5	5.7	15
48	0.09	600	98	2	25	7	5.7	15
49	0.09	815	98	1	25	6	5.7	15
50	0.09	1100	98	2	25	7	5.7	15
51	0.09	600	98	2	25	5	5.7	15
52	0.09	815	98	3	25	5	5.7	15
53	0.09	1100	98	3	25	5	5.7	15
54	0.09	600	98	3	25	6	5.7	15
55	0.09	815	98	3	25	6	5.7	15
56	0.09	1100	98	2	25	6	5.7	15
57	0.09	600	98	3	25	7	5.7	15
58	0.09	815	98	3	25	7	5.7	15
59	0.09	1100	98	3	25	7	5.7	15

Table 12 Experimental results from different welding conditions corresponding to the parameter settings mentioned in Table 11

Exp. no.	UTS	YS	% Elong.	BA	HRD	Exp. no.	UTS	YS	% Elong.	BA	HRD
1	112.08	70.52	9.26	55	51.01	31	2.48	1.69	0.70	5	47.26
2	99.75	58.69	8.72	45	47.77	32	25.50	66.97	1.30	5	46.65
3	116.90	65.65	8.86	60	52.11	33	113.88	59.66	10.66	140	57.80
4	120.28	62.57	21.68	140	47.06	34	121.47	69.51	13.24	140	55.29
5	120.54	62.62	14.66	140	46.23	35	142.23	105.84	16.36	140	62.76
6	114.11	74.58	5.82	140	50.39	36	130.68	80.36	14.92	140	58.55
7	117.19	69.81	7.54	66	51.78	37	129.94	77.85	15.46	140	50.94
8	133.20	63.24	14.60	140	53.82	38	116.66	63.19	14.52	140	53.32
9	94.38	58.61	3.96	45	49.17	39	128.30	79.91	14.94	140	56.13
10	63.28	53.41	3.00	50	47.75	40	125.51	73.05	15.08	140	53.27
11	136.90	72.35	14.8	140	51.24	41	133.89	86.82	15.18	140	49.93
12	112.74	64.25	9.82	10	46.55	42	124.28	70.59	12.71	140	54.57
13	16.01	14.59	0.86	5	49.79	43	129.62	78.97	13.96	140	53.27
14	1.93	1.76	0.76	5	47.26	44	133.05	85.24	15.40	140	50.93
15	138.51	64.47	23.78	140	55.91	45	127.48	75.07	14.01	140	57.31
16	91.72	61.29	4.14	21	46.33	46	132.04	83.37	15.58	140	50.32
17	102.86	69.54	5.60	15	54.29	47	118.50	66.57	12.05	140	56.37
18	94.34	62.74	5.68	25	50.24	48	131.60	84.17	14.34	140	57.93
19	131.00	69.52	17.50	140	52.33	49	125.78	74.71	13.88	140	58.40
20	50.52	49.85	4.34	15	52.23	50	128.52	78.80	14.46	140	55.38
21	64.26	51.72	4.68	10	51.61	51	127.67	75.73	10.26	140	56.11
22	85.09	70.43	3.34	15	52.84	52	133.60	85.65	15.20	140	57.47
23	122.07	57.25	19.28	140	48.61	53	139.73	89.25	16.15	140	58.10
24	117.29	60.76	17.04	140	51.20	54	131.31	84.10	15.06	140	56.09
25	123.68	63.14	10.00	40	48.56	55	135.91	90.74	15.86	140	57.61
26	132.64	63.24	18.26	140	54.29	56	136.22	87.13	16.15	140	53.56
27	91.78	63.54	4.00	10	54.11	57	132.21	87.59	14.62	140	57.64
28	61.52	54.70	1.94	10	51.65	58	135.10	89.25	15.50	140	59.17
29	124.12	63.69	17.46	53	46.83	59	130.53	93.41	15.24	140	54.07
30	126.77	64.09	19.36	140	53.19						

References

Boldsaikhan E, Corwin EM, Logar AM, Arbegast WJ (2011) The use of neural network and discrete Fourier transform for real-time evaluation of friction stir welding. Appl Soft Comput 11(8):4839–4846

Buffa G, Fratini L, Micari F (2012) Mechanical and microstructural properties prediction by artificial neural networks in FSW processes of dual phase titanium alloys. J Manuf Process 14(3):289–296

Deb K (2001) Multi-objective optimization using evolutionary algorithms, 1st edn. Wiley India, New Delhi

Fratini L, Buffa G, Palmeri D (2009) Using a neural network for predicting the average grain size in friction stir welding processes. Comput Struct 87(17–18):1166–1174

Ghetiyaa ND, Patel KM (2014) Prediction of tensile strength in friction stir welded aluminium alloy using artificial neural network. Proc Technol 14:274–281

Haykin S (2003) Neural networks—a comprehensive foundation, 2nd edn. Pearson Education, New Delhi

Kennedy J, Eberhart RC (1995) Particle swarm optimization. In: IEEE international conference on neural networks, ICNN, pp 1942–1948

Lakshminarayanan AK, Balasubramanian V (2009) Comparison of RSM with ANN in predicting tensile strength of friction stir welded AA7039 aluminium alloy joints. Trans Nonferrous Met Soc China 19(1):9–18

Mishra RS, Mahoney MW (2007) Friction stir welding and processing, 1st edn. ASM International, Materials Park

Neto DM, Neto P (2013) Numerical modeling of the friction stir welding process: a literature review. Int J Adv Manuf Technol 65:115–126

Okuyucu H, Kurt A, Arcaklioglu E (2007) Artificial neural network application to the friction stir welding of aluminum plates. Mater Des 28(1):78–84

Shojaeefard MH, Behnagh RA, Akbari M, Givi MKB, Farhani F (2013) Modelling and Pareto optimization of mechanical properties of friction stir welded AA7075/AA5083 butt joints using neural network and particle swarm algorithm. Mater Des 44:190–198

Shojaeefard MH, Akbari M, Asadi P (2014) Multi objective optimization of friction stir welding parameters using FEM and neural network. Int J Precis Eng Manuf 15(11):2351–2356

Storn R, Price K (1997) Differential evolution—a simple and efficient heuristic for global optimization over continuous spaces. J Global Optim 11:341–359

Thomas WM, Nicholas ED, Needham JC, Murch MG, Templesmith P, Dawes CJ (1991) Friction stir welding. International Patent Application PCT/GB92102203, GB Patent Application 9125978.8, 6 Dec 1991

Tutum CC, Hattel JH (2010) A Multi-objective optimization application in friction stir welding: considering thermo-mechanical aspects. In: IEEE congress on evolutionary computation, CEC, pp 1–8